A GCM SIMULATION OF HEAT WAVES, DRY SPELLS, AND THEIR RELATIONSHIPS TO CIRCULATION

RADAN HUTH [1], JAN KYSELÝ [1,2] and LUCIE POKORNÁ [1]

[1] *Institute of Atmospheric Physics, Boční II 1401, 141 31 Praha 4, Czech Republic*
E-mail: huth@ufa.cas.cz
[2] *Department of Meteorology and Environment Protection, Charles University, V Holešovičkách 2, 180 00 Praha 8, Czech Republic*

Abstract. Heat waves and dry spells are analyzed (i) at eight stations in south Moravia (Czech Republic), (ii) in the control ECHAM3 GCM run at the gridpoint closest to the study area, and (iii) in the ECHAM3 GCM run for doubled CO_2 concentrations (scenario A) at the same gridpoint (heat waves only). The GCM outputs are validated both against individual station data and areally representative values. In the control run, the heat waves are too long, appear later in the year, peak at higher temperatures and their numbers are under- (over-) estimated in June and July (in August). The simulated dry spells are too long, and the annual cycle of their occurrence is distorted. Mid-tropospheric circulation, and heat waves and dry spells are linked much less tightly in the control climate than in the observed. Since mid-tropospheric circulation is simulated fairly successfully, we suggest the hypothesis that either the air-mass transformation and local processes are too strong in the model or the simulated advection is too weak. In the scenario A climate, the heat waves become a common phenomenon: warming of 4.5 °C in summer (difference between scenario A and control climates) induces a five-fold increase in the frequency of tropical days and an immense enhancement of extremity of heat waves. The results of the study underline the need for (i) a proper validation of the GCM output before a climate impact study is conducted and (ii) translation of large-scale information from GCMs into local scales using downscaling and stochastic modelling techniques in order to reduce GCMs' biases.

1. Introduction

Ecosystems and various sectors of human activities are particularly sensitive to extreme climate phenomena, including heavy rains, droughts, high and low temperatures. Even relatively small changes in means and variations of relevant climate variables can induce considerable changes in the severity of extreme events (Katz and Brown, 1992; Hennessy and Pittock, 1995). Such changes are likely to have a great impact on ecosystems and society. Of particular importance are long-lasting extreme events, such as prolonged periods with no precipitation (dry spells) and with high temperatures (heat waves), both imposing high stress on plants, animals and humans. Heat waves and dry spells are the focus of this study.

Among a variety of harmful effects, episodes of extremely high temperatures can damage plants, especially when there is a shortage of water (Kirschbaum, 1996), which can adversely affect their growth during key development stages

Climatic Change **46:** 29–60, 2000.
© 2000 *Kluwer Academic Publishers. Printed in the Netherlands.*

(Acock and Acock, 1993). Heat stress has detrimental effects also on livestock with significant impacts on milk production, as well as on reproductive capabilities of dairy bulls and conception in cows (Thatcher, 1974; Cavestany et al., 1985; Furquay, 1989). Heat waves pose a danger for human health, too, and during heat waves, the overall death rates rise (Kalkstein and Smoyer, 1993; Kunst et al., 1993; Changnon et al., 1996). The prolonged periods with no precipitation may cause a soil moisture deficit, which impairs crops as consistent moisture availability throughout the growth period is critical for them (Reilly, 1996).

General Circulation Model (GCM) studies have recently paid increased attention to extreme phenomena, both in validating simulated present-day climates and analyzing possible future climates. For example, Joubert et al. (1996) and Mason and Joubert (1997) analyzed frequencies of droughts and extreme rainfall events in South Africa in the CSIRO GCM. Hennessy et al. (1997) examined the probability of exceeding precipitation thresholds in two GCMs at various locations. Gregory et al. (1997) dealt with dry spells and their return periods in the transient experiment with the Hadley Centre GCM.

The climate variables on a local scale are to a certain extent (widely differing among variables) governed or influenced by large-scale circulation. The heat waves and dry spells do not therefore occur independently of circulation conditions, but their occurrence is favoured by certain flow configurations while unlikely under other ones. The relationship between circulation and the occurrence of prolonged extreme events is thus an important component of a climate system, and the accuracy with which it is simulated by a GCM can serve as one of indicators of the model's validity. For example, Risbey and Stone (1996) found that circulation conditions producing high precipitation events differ between the model and reality, precipitation being caused by different mechanisms. Heat waves and dry spells have not been examined from this point of view yet.

The present paper investigates heat waves and dry spells observed in south Moravia (southeastern part of the Czech Republic) during the vegetation period, and their relationships with continental-scale circulation. The observations are compared with the corresponding ECHAM GCM simulations both for present climate and for doubled CO_2 concentrations.

When validating a GCM output on a local scale, one should bear in mind that GCMs have not been designed for simulating local climate. The interpretation of GCM outputs is, therefore, ambiguous: The values at GCM's gridpoints can be treated in two alternative ways, either as areal or point quantities. In terms of GCM validation, i.e., comparing simulated and observed values, this means that GCM gridpoint values should be compared either with area-averaged observations or directly with local values. There is continuing debate, about which approach should be given preference and considered more appropriate, but still without a definitive conclusion (Skelly and Henderson-Sellers, 1996; Zwiers and Kharin, 1998). Some studies have compared GCM outputs with observations at individual stations (Portman et al., 1992; Palutikof et al., 1997; Schubert, 1998; Nemešová

et al., 1998, to name a few), others with observations interpolated to gridpoints or with gridded climatologies (e.g., Airey and Hulme, 1995; Risbey and Stone, 1996; Osborn and Hulme, 1998). The dilemma is perhaps more serious for precipitation, which is more spatially variable, and whose spatial behaviour widely changes from seasons and regions with prevailing stratiform rainfall to those with convective rainfall. Robinson et al. (1993) have shown that during the convective season, the GCM-simulated number of dry days closely approximated the individual station values, whereas during the seasons with prevailing stratiform precipitation, it was closer to the areal aggregate value.

Nevertheless, the approach to validation is frequently selected arbitrarily, which is only sometimes explicitly admitted (e.g., by Osborn and Hulme, 1998). In this paper, the GCM outputs are validated against the individual station values and two kinds of area-representative variables: (i) the 'pooled' ones obtained by averaging the heat wave and dry spell characteristics, calculated at individual stations, and (ii) the 'averaged' or 'aggregated' ones, obtained by calculating the characteristics from area-averaged or aggregated series. Whereas the pooled values can be thought of as characteristics at a 'typical' single station, the averaged (aggregated) values describe the behaviour of area-averaged temperature and precipitation, forming an analogy to a GCM output treated as a gridbox value.

Recent examinations of the ECHAM GCM revealed that its precipitation climatology is simulated worse than its temperature climatology in the region considered. Specifically, the model systematically underestimates the interdiurnal variability of temperature and is too wet (Nemešová and Kalvová, 1997; Kalvová and Nemešová, 1998; Nemešová et al., 1998).

2. Data

This study examines the heat waves and dry spells during the vegetation period, which in central Europe covers approximately the months from March to October. Three datasets are analyzed: observations, the ECHAM simulation of the present climate (control run; CTR), and the equilibrium ECHAM simulation of the climate under doubled CO_2 concentrations (scenario A run; SCA). The simulated datasets were produced by the ECHAM3 model with the T42 resolution, corresponding approximately to a 2.8° gridstep both in longitude and latitude. In the control run, the climatological SSTs and sea ice were employed while the scenario A equilibrium run was forced by SSTs and sea ice averaged over years 65 to 74 (roughly corresponding to doubling CO_2) in the scenario A transient integration. The model is described in detail in DKRZ (1993). Each dataset comprises thirty years. Observations span the period 1961–1990; in the simulations, years 11 to 40 in the control run and years 13 to 42 in the scenario run are analyzed. Each model month consists of 30 days. The observations thus amount to 7350 days, and CTR and SCA data to 7200 days.

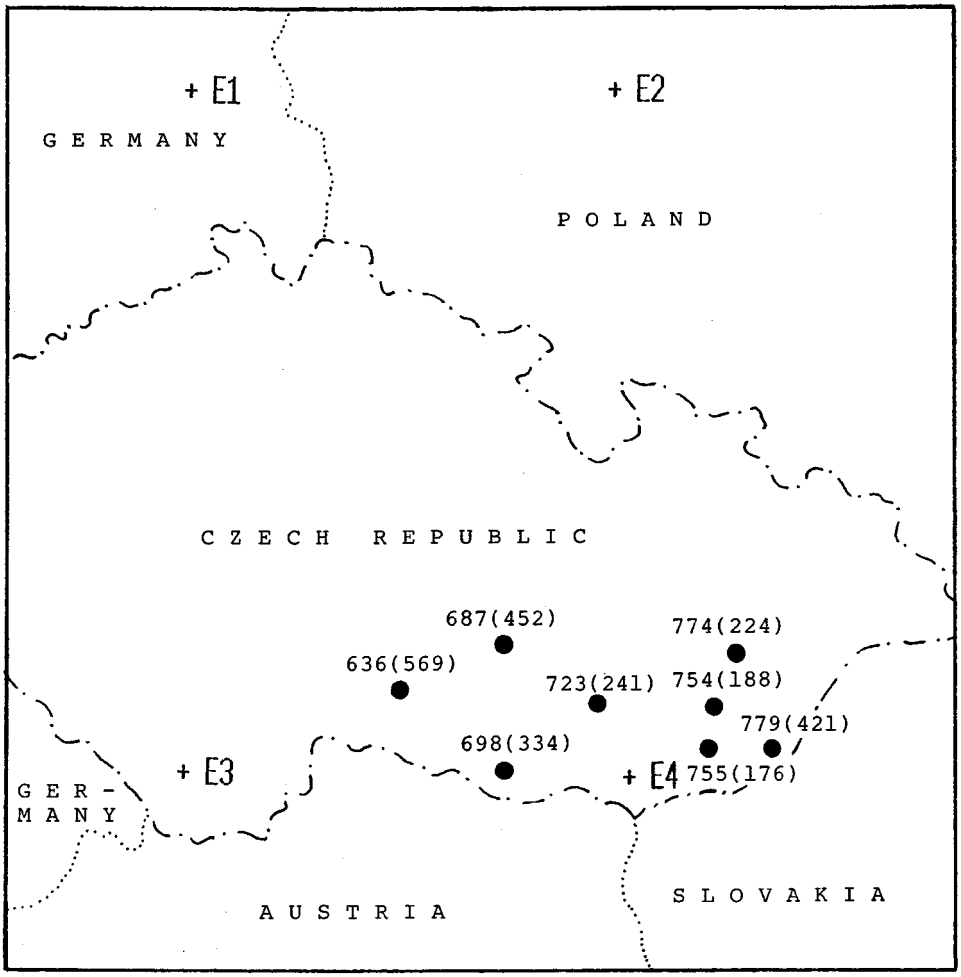

Figure 1. Location of stations used in the study (dots) and ECHAM GCM grid points (crosses). Stations are identified by their numbers, with their altitudes (in m a.s.l.) given in parentheses.

The observed maximum temperatures and precipitation are analyzed at eight south Moravian stations (Moravia is the eastern part of the Czech Republic). Figure 1 shows their locations and altitudes together with the position of the close ECHAM gridpoints. Because of similarity of basic characteristics of simulated temperature and precipitation time series at the four close gridpoints (Kalvová and Nemešová, 1998; Nemešová et al., 1998), point E4, nearest to the region analyzed, was taken as a representative of south Moravia in the model.

Continental-scale circulation is characterized by 500 hPa geopotential heights. The observed values were interpolated using bicubic splines from the $5° \times 5°$ grid onto the model grid (approximately $2.8° \times 2.8°$), covering most of Europe and

the easternmost flank of the Atlantic Ocean. For the area covered by the grid, see Figure 5 as an example.

3. Heat Waves

There are two general approaches to defining heat waves: Either the most extreme events lasting the period of a required duration (typically one to three days) in each summer are selected or all heat waves above a certain threshold are analyzed (Karl and Knight, 1997). Here we adopted the latter approach as it allows us to consider several heat waves in one year. Possible definitions of what can be considered a heat wave differ according to the thresholds employed, for example, in its required duration and extremity. We found it useful to define the heat wave as 'the longest continuous period (i) during which the maximum daily temperature reached at least T_1 in at least three days, (ii) whose mean maximum daily temperature was at least T_1, and (iii) during which the maximum daily temperature did not drop below T_2'. The threshold temperatures T_1 and T_2 are set to 30° and 25 °C, respectively, in observations. This is in accordance with common climatological practice in the Czech Republic, which refers to the days with maximum temperature reaching or exceeding 30° and 25 °C as tropical and summer days, respectively. The definition follows the general perception of what a heat wave is: It allows two periods of tropical days separated by a slight drop of temperature to compose one heat wave but, on the other hand, two periods of tropical days separated by a pronounced temperature drop below 25 °C (e.g., due to a cold front passage) are treated as separate heat waves. The minimum duration of a heat wave required by the definition is three days.

Given the definition for observed data, there are two ways of defining the heat wave in the GCM control simulation. Either the thresholds of 30° and 25 °C can be directly applied or the thresholds can be redefined in the control run so that the probability of exceeding them would be the same as in the observed. The latter way accounts for the model's possible temperature bias, thereby allowing a more direct interpretation of the scenario run, and has therefore been applied in this study. The respective percentiles of the maximum temperature distributions corresponding to 30° and 25 °C thresholds were determined at the eight stations for the period from May to September. Their values representative for the region were obtained by averaging the eight local percentiles: They equal 97.1% and 80.9%, respectively, for 30° and 25 °C temperatures. In the simulated maximum temperature distribution at point E4, the two percentiles coincide with temperatures of 30.7° and 24.5 °C. This procedure is referred to as 'averaged-percentiles' (AP) adjustment. An alternative to it is to take the time series of area-averaged values as a basis ('averaged-temperature' – AT adjustment): The areal mean temperature of 30 °C and 25 °C corresponds to the percentiles of 97.7% and 82.0%, respectively, in its distribution; the adjusted threshold temperatures in the control simulation then

being 31.2 °C and 24.7 °C. Both ways of adjusting simulated thresholds lead to the values that correspond relatively well to the observed thresholds, indicating that the right tail of the maximum temperature distribution is simulated by the model rather successfully, even though it is notably flatter relative to observations. In the two simulated climates, the terms 'summer day' and 'tropical day' refer to the adjusted threshold temperatures.

Basic characteristics of heat waves are summarized in Table I for individual stations and gridpoint E4. Also shown are the characteristics pooled over all the stations, and over the lowland and higher-elevated stations separately, as well as the characteristics for the spatially averaged temperature series. The heat waves are characterized by their total occurrence in 30 years, average peak day (the peak day is the central day of the three-day period with highest mean maximum temperature within a particular heat wave), average duration, peak temperature (the highest maximum temperature of a heat wave), relative position of the peak within the heat wave (defined as a ratio between the order of the peak day within the heat wave and its duration), and the percentage of all tropical days that occur in heat waves.

A detailed scrutiny of the observed heat waves was performed by Kyselý and Kalvová (1998). Here we only note a pronounced dependence of several characteristics on elevation: at higher elevations, the heat waves are less frequent, tend to peak later and to be shorter, and the percentage of tropical days that occur in heat waves is smaller. The peak temperature and the relative position of the peak appear to be independent of elevation. The heat wave characteristics calculated from the averaged temperature series (AVG) closely resemble the characteristics averaged over individual stations (ALL). The only exception is the relative position of the heat wave peak, which in the averaged temperatures is shifted to the center of heat waves.

The AT adjustment results in a bit higher threshold temperatures, so the two adjustments lead to slightly different heat wave characteristics in the control climate: the mean duration is shorter and peak temperature higher for the AT adjustment. The most important finding is, however, a disparity between the control and observed heat wave characteristics, regardless of how they are defined. The heat wave frequency and the relative position of the peak in the control simulation compare quite well with the observations; however, these are the only two quantities that are reproduced successfully by the model. The simulated heat waves are much longer than the observed, tend to occur later, and peak at temperatures by about 2 °C higher. Also, fewer tropical days occur outside of heat waves. Most of these discrepancies result from two shortcomings of the model, viz., too low an interdiurnal variability (Nemešová and Kalvová, 1997) and a deformation of the temperature annual cycle with a maximum shifted towards August (see Figure 2 where the annual cycles of the mean temperature are shown for the eight stations and two model runs).

The character of heat waves changes dramatically in the scenario climate. The model indicates that the mean monthly temperature at point E4 increases due to

TABLE I

Characteristics of heat waves: total number in 30 years; average peak day (day/month), duration (days), peak temperature (°C), and relative position of the peak within the heat wave (ratio between the order of the peak day within the heat wave and its duration); and the percentage of tropical days that occur in heat waves. Values are given for individual stations (636 to 779), pooled over lowland (LO), higher-elevated (HI) and all (ALL) stations, for spatially averaged temperature (AVG), and for the control (CTR) and scenario (SCA) climates at point E4. The higher-elevated stations are 636, 687 and 779, the lowland stations include the other five. The values for simulated climates are shown for both threshold adjustments (AP and AT – see text for definitions)

	636	687	698	723	754	755	774	779	LO	HI	ALL	AVG	CTR AP	CTR AT	SCA AP	SCA AT
Number	9	16	28	32	37	43	30	11	34	12	26	22	24	22	53	52
Peak day	4/8	25/7	27/7	30/7	24/7	25/7	26/7	1/8	26/7	31/7	28/7	30/7	9/8	8/8	3/8	5/8
Duration	5.3	5.9	7.8	7.2	7.4	6.8	6.4	5.3	7.1	5.5	6.5	6.6	11.3	9.7	34.8	33.7
Peak temp.	32.9	32.7	33.3	32.5	32.8	32.6	32.4	32.0	32.7	32.5	32.6	32.5	34.4	34.7	37.8	37.9
Position	0.76	0.63	0.68	0.71	0.63	0.63	0.67	0.60	0.66	0.66	0.66	0.59	0.62	0.62	0.58	0.57
Percentage	39.5	42.7	57.3	63.0	63.3	66.1	59.6	43.3	62.2	42.0	58.0	58.4	82.3	81.0	97.4	97.1

TABLE II

Mean monthly and annual frequency of tropical days. The observed data are adjusted so that they correspond to a 30-day month. The notation of columns is same as in Table I. There are no tropical days in the months not shown (October to April) at any station/in any climate

Month	636	687	698	723	754	755	774	779	LO	HI	ALL	AVG	CTR AP	CTR AT	SCA AP	SCA AT
V	0.0	0.0	–	–	0.0	0.1	0.0	–	0.0	0.0	0.0	0.0	–	–	–	–
VI	0.1	0.6	0.8	0.9	1.5	1.5	1.1	0.3	1.1	0.3	0.8	0.6	0.2	0.1	2.6	2.3
VII	1.1	2.2	3.3	3.2	3.7	3.7	2.8	1.3	3.3	1.5	2.7	2.2	1.5	1.4	12.9	12.2
VIII	1.2	1.8	2.9	2.9	3.4	3.7	2.7	1.4	3.1	1.4	2.5	1.9	3.9	3.0	20.0	19.4
IX	0.1	0.2	0.3	0.3	0.4	0.4	0.2	–	0.3	0.1	0.2	0.1	0.5	0.3	4.4	3.9
Annual	2.5	4.8	7.3	7.3	9.0	9.4	6.8	3.0	8.0	3.4	6.3	4.9	6.1	4.9	39.9	37.9

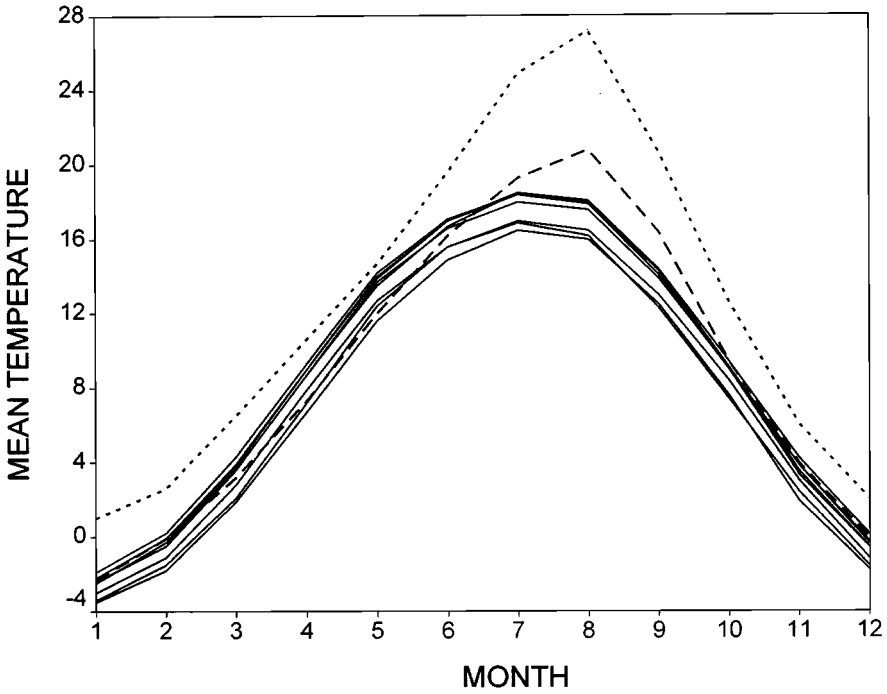

Figure 2. Annual cycle of mean temperature at eight stations (solid lines) and at point E4 in the control (dashed) and scenario (dotted) climate.

doubling CO_2 concentrations by 3.4 °C in June, 5.6 °C in July and even 6.4 °C in August (Figure 2). This leads to an immense increase in the number of tropical days: five to six tropical days per year occur in the control climate (depending on the threshold definition), which is in accord with observations, while in the scenario climate, this number rises up to 40 (last row in Table II). As a consequence, the number of heat waves is more than doubled, the average heat wave lasts longer than a month and its peak temperature reaches almost 38 °C (Table I). Tropical days outside of heat waves become an exception. There are heat waves in the scenario run that last more than 80 days, starting in mid-June and persisting until early September. The most extreme heat wave peaks at 46 °C, maximum temperature not dropping below 40 °C during seven successive days.

The deformation of the maximum temperature annual cycle in the model can be illustrated by the frequency of tropical days in individual months (Table II). Tropical days are most frequent in July in all the observed series (including the averaged ones), except for two elevated stations, 636 and 779, where a slight dominance of tropical days in August is found. In the control simulation, a strong maximum in the number of tropical days occurs in August. The model clearly underestimates the number of tropical days in late spring and early summer (May–July) but exaggerates it in late summer and early autumn (August, September). This

TABLE III

Mean monthly and annual frequency of tropical days in heat waves. The values for individual stations are not shown; otherwise as in Table II

Month	LO	HI	ALL	AVG	CTR AP	CTR AT	SCA AP	SCA AT
V	–	–	–	–	–	–	–	–
VI	0.5	0.1	0.4	0.1	0.2	0.1	2.3	1.9
VII	2.3	0.7	1.7	1.5	1.2	1.1	12.6	11.9
VIII	2.0	0.6	1.4	1.1	3.1	2.6	19.8	19.2
IX	0.1	0.1	0.1	0.1	0.5	0.2	4.2	3.7
Annual	5.0	1.4	3.6	2.8	5.0	4.0	38.9	36.8

unrealistic feature, i.e., the shift of the annual temperature maximum to August, is retained in the scenario run: the number of tropical days in August highly exceeds that in July.

Despite the deformation of the seasonal cycle, the heat waves occur in the same months in the control run as in observations, i.e., in June to September (Table III). An interesting feature is that although the thermal extremity increases in the scenario run in all aspects (number of tropical days, number and duration of heat waves), the heat waves do not spread further to spring and autumn and their occurrence remains limited to the period from June to September.

The conclusions concerning the simulated heat waves do not appear to be sensitive to what they are compared with: both the characteristics of the spatially averaged temperature and the pooled characteristics yield similar results, which differ widely from the control simulation. Most characteristics of control heat waves fall well outside the range of values observed at individual stations. On the other hand, the results for the control climate are robust regarding the definition of threshold temperatures. In other words, the validation of heat waves appears to be insensitive to whether the GCM output is treated as gridpoint or gridbox value.

4. Dry Spells

Dry spells are usually defined as runs of consecutive days without precipitation. In many applications, however, it is common to allow days with very small precipitation amounts to be considered as dry and to be included in dry spells (e.g., Joubert et al., 1996; Gregory et al., 1997). In this study, we define a dry spell as the longest continuous period lasting 10 days or more, during which the precipitation total does not exceed 1 mm.

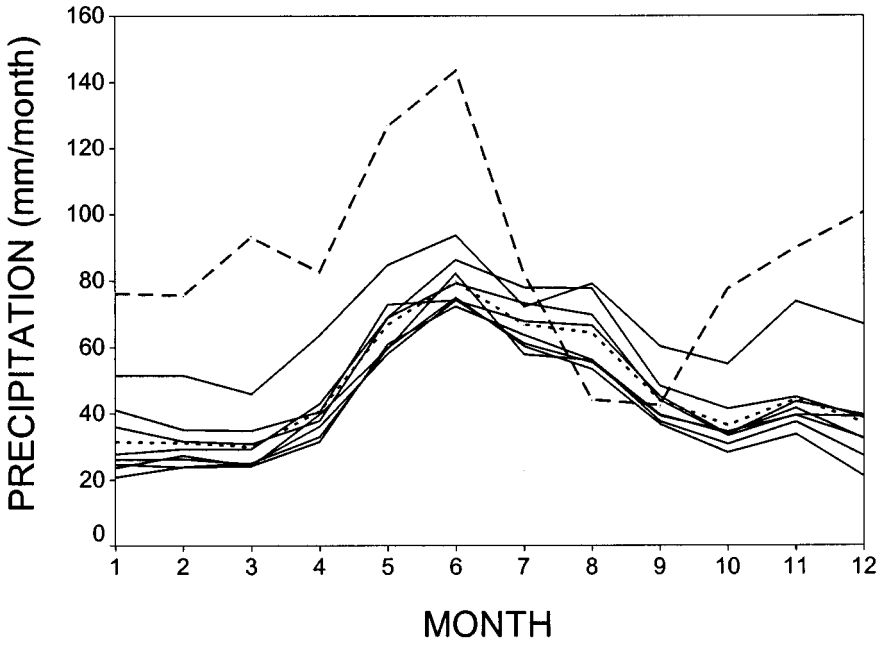

Figure 3. Annual cycle of monthly precipitation totals at eight stations (solid lines), their areal average (dotted), and at point E4 in the control climate (dashed).

Because of large spatial variability, constructing areal representation (aggregate value) of precipitation is a difficult task. Following Robinson et al. (1993), the 'aggregate dry day' can be defined as the day when no precipitation was recorded at any station. This is a rather stringent definition, especially during the convective season when local showers that are recorded at only a single station may be quite frequent. Therefore, we employ another, more liberal, criterion, whereby we count days with precipitation recorded at just one station as 'aggregate dry days'. The two criteria are referred to as 'aggregate (0)' and 'aggregate (1)', respectively, in the text below.

To be able to calculate 'aggregate dry spells', one has to define the area-averaged precipitation series. Here, we define it simply as an average of station values.

The analysis is confined to the observed and control climates, since for the scenario climate, precipitation values were unfortunately not available.

Let us start with monthly precipitation sums. There is a wide difference in annual cycle between the observed and control climate, the latter appearing to be unrealistic (Figure 3). The observed precipitation series agree with each other in having their annual maximum in early summer and minimum in winter; a secondary minimum and maximum appear in October and November, respectively. The control annual cycle is clearly bimodal with maxima in June and December and main minimum in August and September. The annual precipitation sum is

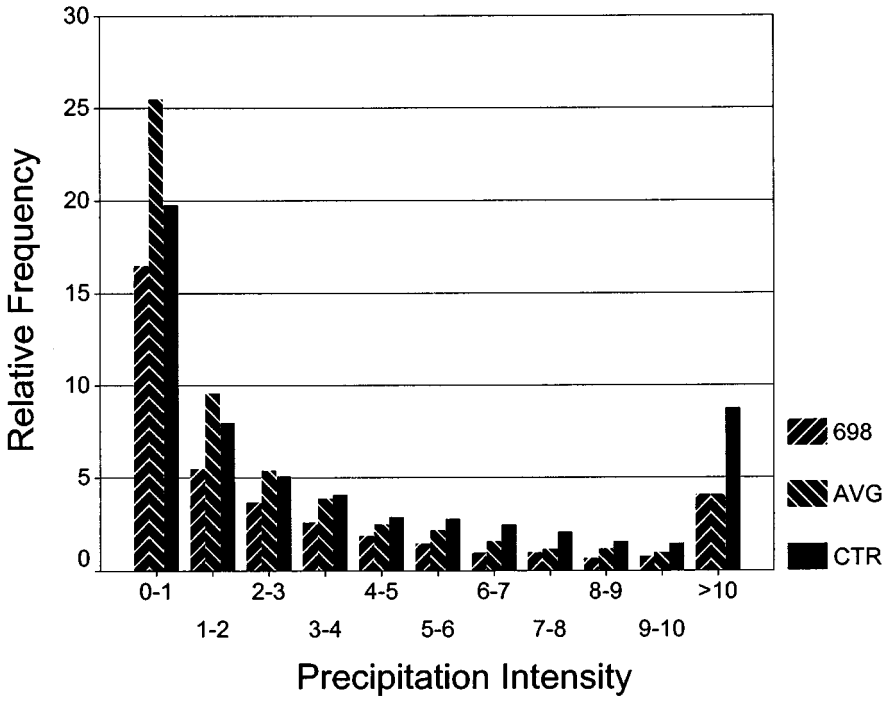

Figure 4. Relative frequency of daily precipitation totals for station 698, areal average (AVG), and control run at point E4 (CTR). Relative frequency of dry days (not included in the figure) is 60.8% for station 698, 41.6% for the areal average, and 40.8% for the control run.

exaggerated in the model by a factor of more than two. The only two months when the model delivers less precipitation than observed at any station are August and September; the overestimation is largest in winter.

Two systematic errors may be the source of the excessive wetness of the control climate: the number of days without precipitation may be too low and/or the precipitation intensity too high. Which error is in effect can be deduced from the precipitation frequency distributions (Figure 4). First of all, we should note a difference between the observed values at a single station and the area-averaged values: at a single station, the share of days without precipitation is much larger than for the average series, whereas for all non-zero precipitation intensities, the share at a single station is smaller. The higher the intensity, the closer the single station and area-averaged values. The comparison of precipitation intensity frequencies in the control climate with observations at a single station appears to be inadequate: The control intensities are closer to the area-averaged values. The number of dry days is almost the same (around 41%) in the areally averaged observations and the control climate. However, the model overestimates the number of rainy days for moderate and heavy precipitation (over 3 mm). This is an important difference from a ‘drizzly’ nature of other models, which tend to overestimate the frequency

of light precipitation but underestimate heavier rains (e.g., Reed, 1986; Risbey and Stone, 1996).

Basic characteristics of the distribution of dry spells duration (mean, median, maximum) as well as their mean annual frequency and the percentage of dry days that occur in dry spells are listed in Table IV. Shown are the values for the eight stations, values averaged over the lowland, higher-elevated and all stations, the values for the area-averaged precipitation, and values for the control climate at point E4. There is little difference in the characteristics of dry spells duration (mean, median, maximum) between individual stations and the area-averaged values, and between lowland and highland stations. For the area-averaged precipitation, the annual frequency of dry spells is much lower than at individual stations, and there is much weaker tendency for dry days to chain in prolonged spells. It is also worth noting that at lowland stations, the dry spells are more frequent and relatively more days occur within dry spells than at higher-elevated stations. In the control climate, dry spells are longer than in the observed. Since the dry spells duration distributions for the observed and control climate have the same median but differ in their means, we can state that the model overestimates the frequency of very long spells at the expense of spells with medium duration (13 to 20 days). The frequency of dry spells in the control climate compares fairly well with the observed area-averaged precipitation; on the other hand, the simulated percentage of dry days occurring within dry spells resembles the single station values.

The observed and control climates differ notably in the distribution of dry days and dry spells throughout the year. In the observed, the number of days within dry spells (Table V) closely reflects the annual cycle of precipitation: the larger the precipitation total, the fewer days within dry spells. This holds both for area-averaged precipitation, and precipitation at individual stations, represented by the pooled values. In the control climate, such a simple relationship does not hold. The number of days within dry spells peaks in the driest months of August and September, which corresponds to the minimum of the precipitation annual cycle. However, dry spells are rarest in spring even though March, April and May are all less wet than the month with maximum precipitation, i.e., June. Although the March and April precipitation amounts are comparable with July and October, the dry spells in spring are much less frequent. The total simulated frequency of dry days in the vegetation period (Table VI) is closest to the number of aggregate dry days according to criterion (1) (which allows the day with precipitation at one station to be counted as dry). However, the annual cycles are very different: The frequency of dry days varies rather moderately in the observed, with the minimum in June and maximum in October. In the control climate, the range is much broader: dry days are least frequent in March (although March is far from being the wettest month) with less than six dry days on average whereas more than 21 dry days occur in August and September.

The percentage of dry days occurring in dry spells is almost the same in the control climate as at individual stations if the vegetation period is considered as

TABLE IV

Characteristics of dry spells: mean, median and maximum duration, mean annual frequency, and percentage of all dry days that occur in dry spells. Given are values for eight individual stations, the values pooled over five lowland (LO), three higher-elevated (HI), and all (ALL) stations, the values for precipitation series averaged over lowland, higher-elevated, and all stations, and the values for the control run. For the area-averaged precipitation, the percentage is calculated for the aggregate dry days according to criterion (0), i.e., with no precipitation at any station

	Stations								Pooled			Averaged			CTR
	636	687	698	723	754	755	774	779	LO	HI	ALL	LO	HI	ALL	
Mean	13.8	14.1	14.8	14.6	14.5	14.9	13.8	14.0	14.5	14.0	14.3	14.2	14.0	13.7	18.1
Median	13	12	13	13	13	13	12	12	13	12	13	12	12	12	13
Maximum	34	36	34	38	38	38	31	34	36	38	38	35	34	34	49
Frequency	4.2	4.0	5.0	5.7	5.0	4.9	4.7	4.7	5.1	4.3	4.8	4.0	2.9	3.1	2.8
Percentage	38.1	37.6	45.1	48.6	45.7	44.5	41.9	38.2	45.2	38.0	42.6	24.9	20.0	22.0	42.5

TABLE V

Mean monthly and total (for the vegetation period) number of days within dry spells: values pooled over all stations (POOL), for area-averaged precipitation (AVG), and for control climate (CTR)

Month	POOL	AVG	CTR
III	10.2	3.8	0.7
IV	10.2	5.6	1.8
V	5.1	1.8	0.8
VI	3.5	1.3	1.9
VII	5.4	2.2	4.6
VIII	6.8	1.9	15.3
IX	10.8	7.0	15.3
X	14.0	11.7	5.1
Total	66.0	37.4	45.5

a whole (bottom row in Table IV). However, the climates differ widely in this quantity if compared month by month (Table VII). For example in dry months, the tendency towards chaining dry days in long periods without rain is similar

TABLE VI

Mean monthly frequency of dry days and their total in the vegetation period. AGGR(0) and AGGR(1) refers to the two definitions of the 'aggregate dry day', given in the text

Month	POOL	AGGR(0)	AGGR(1)	CTR
III	17.3	10.4	13.7	5.8
IV	17.9	11.2	13.5	11.4
V	16.4	9.3	12.8	9.4
VI	15.5	8.2	10.8	8.8
VII	17.2	10.6	13.9	14.1
VIII	18.1	11.7	14.5	21.2
IX	19.2	11.5	15.5	21.7
X	19.5	11.1	15.9	14.7
Total	141.1	84.0	110.6	107.1

TABLE VII

Percentage of dry days occurring in dry spells, monthly values. Otherwise as in Table VI

Month	POOL	AGGR(0)	AGGR(1)	CTR
III	59.0	37.6	33.4	12.1
IV	57.0	36.2	32.6	15.8
V	31.1	14.7	12.7	8.5
VI	22.6	11.9	10.5	21.6
VII	31.4	16.9	14.1	32.6
VIII	37.6	12.4	12.4	72.2
IX	56.2	41.0	38.6	70.5
X	71.8	56.8	56.7	34.7

in the control climate (August and September) to the observed in October but considerably stronger than in the observed in spring (March and April).

5. Circulation

Before validating relationships of heat waves and dry spells to continental-scale circulation, we should examine circulation itself. In doing so, we follow the methodology used in Huth (1997a) where continental-scale circulation is characterized in two complementary ways, namely, by modes of variability and by circulation types.

Modes of variability are identified in two important frequency bands: (i) synoptic frequencies, in which synoptic-scale pressure formations (cyclones, anticyclones), affecting in midlatitudes the instantaneous weather conditions and their day-to-day changes, develop and move, and (ii) low frequencies, in which planetary-scale formations such as blocking events evolve, affecting weather conditions over large areas for relatively long time periods. For this purpose, 500 hPa heights were filtered using Blackmon and Lau's (1980) low-pass and band-pass filters, which retain periods longer than 10 days (low frequencies) and 2.5 to 6 days (synoptic frequencies), respectively. As an analysis tool, obliquely rotated principal component analysis (PCA) in an S-mode is used. The procedure is basically the same as in Huth (1997a) where it is described in detail.

The modes of variability identified in the three datasets are displayed in Figures 5 (low frequencies) and 6 (synoptic frequencies) in terms of principal component (PC) loadings. PC loadings are correlations of PC amplitudes with original (low-passed or band-passed) data. Circulation on each day in respective frequency bands can be approximated by a linear combination of the modes detected. For example,

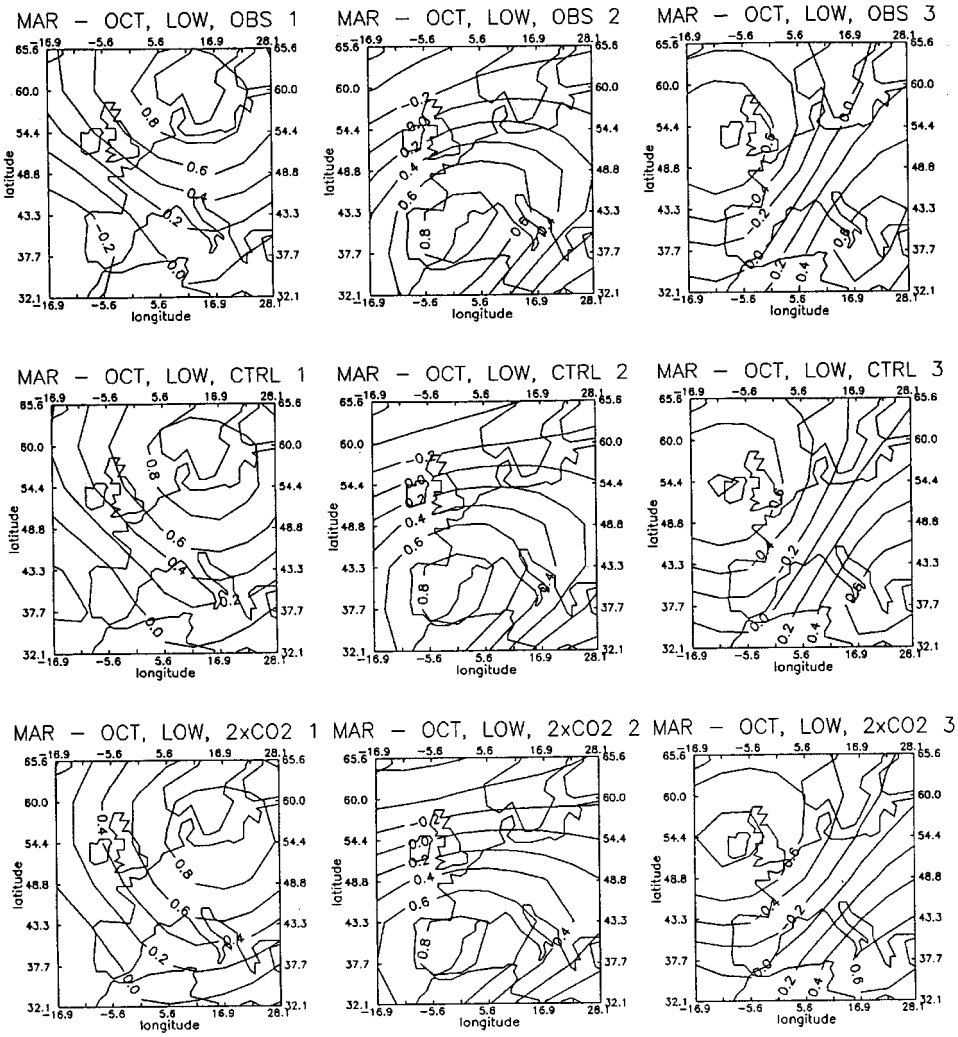

Figure 5. Modes of low-frequency variability (i.e., correlations between principal components and 500 hPa geopotential heights): observed (top), control (middle) and scenario (bottom).

days with positive amplitudes of the third low-frequency PC are remarked by a negative anomaly over and west of the British Isles and a positive anomaly centered over central Mediterranean, inducing a southwest flow in central Europe, whereas negative amplitudes of PC 3 cause a north to northeast flow in central Europe.

There is a clear one-to-one correspondence between the low-frequency modes detected in the observed, control, and scenario datasets. There are minor differences, e.g., in the position of the Scandinavian center in mode 1 and in the orientation of the anomaly flow in modes 2 and 3; in spite of it we can state that the low-frequency variability is captured very well by the ECHAM GCM. A one-

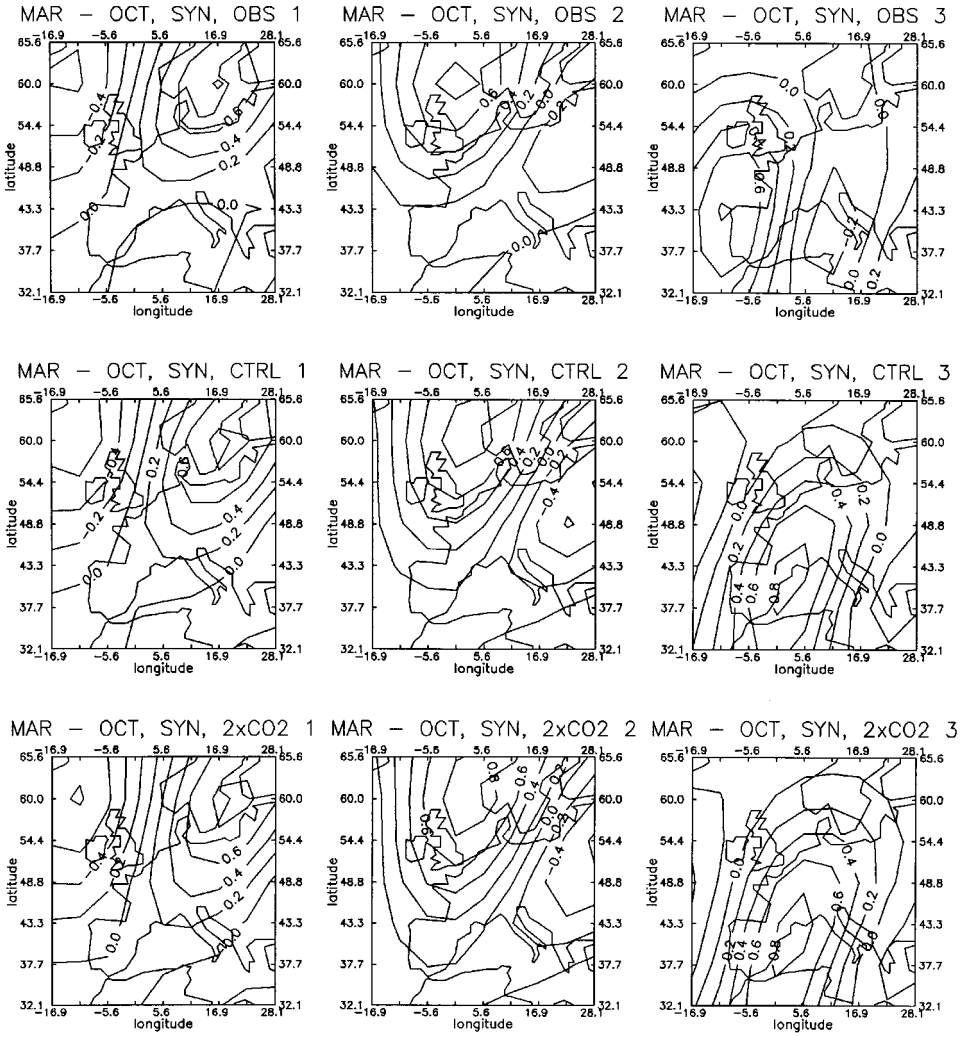

Figure 6. Modes of synoptic-frequency variability; otherwise as in Figure 5.

to-one correspondence can also be found for synoptic-frequency modes, that is, the variability in synoptic band is also well simulated by the model. (Note that observed mode 3 is paired with control and scenario mode 4, and vice versa.) The modes of variability in both frequency bands differ negligibly between the control and scenario climates. This indicates that the enhanced greenhouse effect will, according to the ECHAM GCM, cause only a marginal change in the modes of variability.

In identifying circulation types, we followed a modified methodology of Huth (1997a); please refer therein for more details on the procedures used. The PCA in a T-mode was applied to a subset of the observed dataset, consisting of every

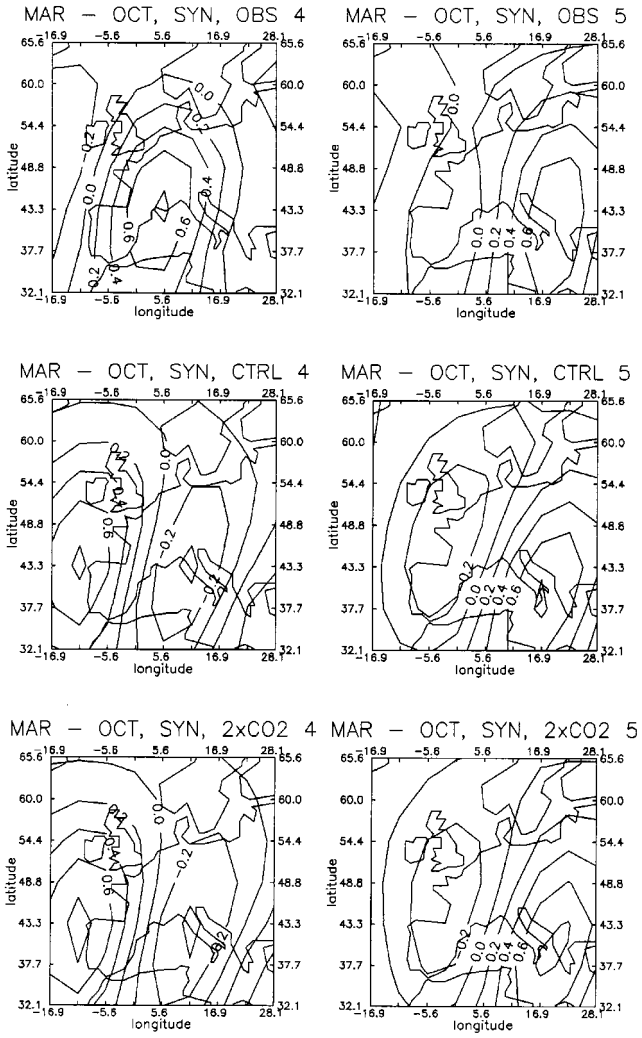

Figure 6. (Continued).

fifteenth daily pattern. This resulted in prerequisite circulation types. They were then projected on the whole observed dataset, as well as on the two model datasets. The projection is a mathematical operation, which, simply speaking, consists in assigning a pattern to the prerequisite type most similar to it. The projection makes it possible to cope with large datasets and allows a fair comparison between observed and simulated types. Its description in mathematical terms can be found in the paper by Huth (1997a). All daily patterns are classified unambiguously, i.e., with just one type.

Six circulation types were identified in the observed data and, because of the projection, the same types were analyzed also in the control and scenario model

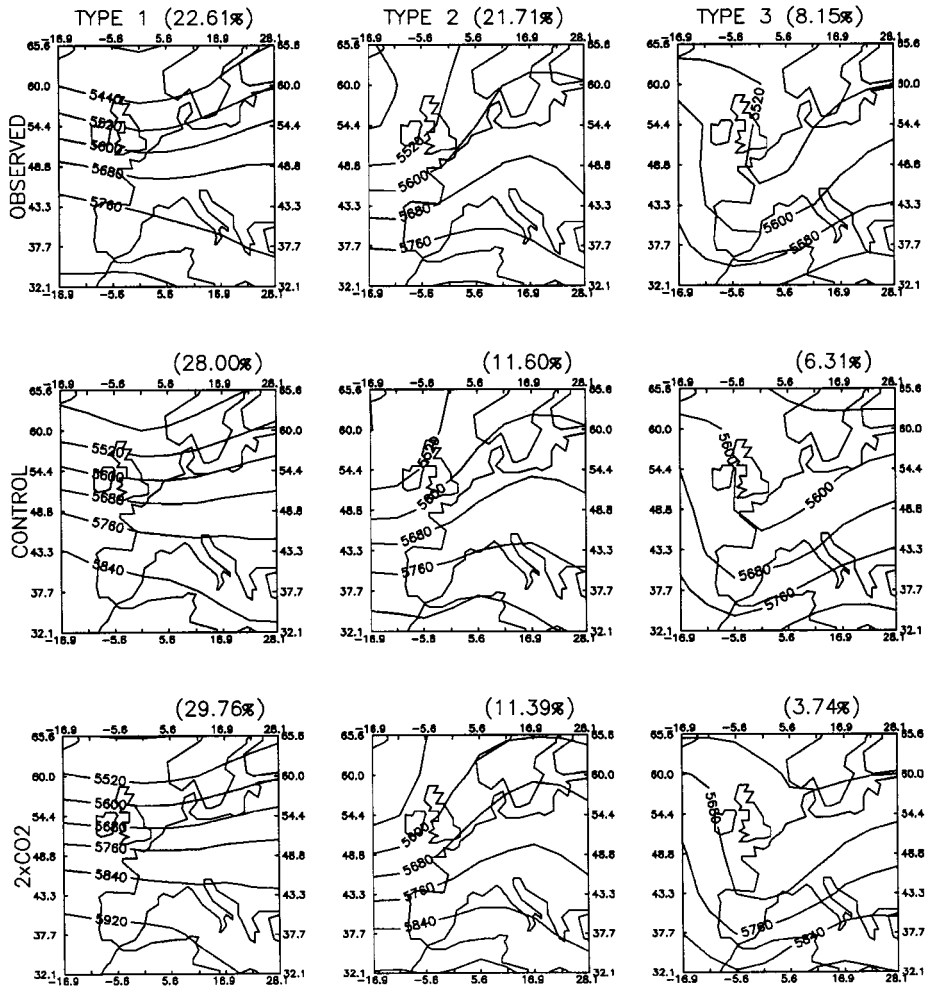

Figure 7. Mean 500 hPa height patterns (in metres) of the circulation types: observed (top), control (middle) and scenario (bottom). The percentage of occurrence of each type is given in parentheses.

runs. The mean 500 hPa height patterns for all the types in the three datasets are shown in Figure 7. Several features are worth noting. First, some types are simulated with incorrect frequency: the types 1 (zonal flow), 4 (ridge over Britain) and 6 (jet displaced far northwards) are too frequent in the model, whereas the frequency of type 2 (broad ridge over Europe) is strongly underestimated. Second, some simulated types have slightly distorted patterns, e.g., the trough of type 3 is too weak in the control climate. Analogous differences can be found between the control and scenario climates, the most striking features being the increased frequency of days with jet displaced northwards (type 6) and decreased frequency of troughs over western Europe (type 3).

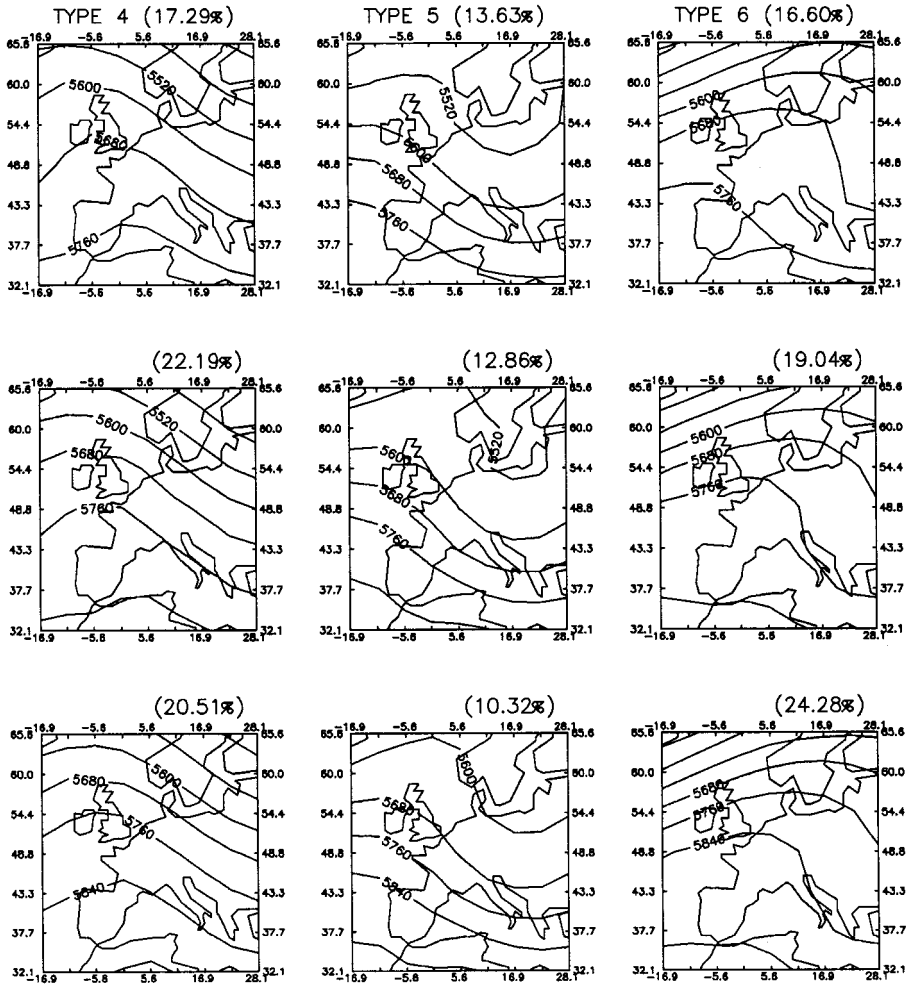

Figure 7. (Continued).

The persistence of the model circulation was assessed in terms of average duration of circulation events, i.e., periods of days classified with one type, preceded and succeeded by another type (Table VIII). The average duration of events (regardless of circulation types) is simulated correctly. Differences between the observed and control climate appear, however, once the circulation types are treated individually: the model overestimates persistence of types 1 (zonal flow) and 4 (ridge over Britain) whereas strongly underestimates persistence of type 2 (broad ridge over Europe). Circulation in the scenario climate is slightly less persistent in general, the decrease in persistence being most pronounced for types 2–4.

Generally speaking, the ECHAM GCM is relatively successful in simulating continental-scale circulation over Europe, the most notable deficiency of the control climate being the lack of broad ridges over Europe.

TABLE VIII

Average duration of circulation events (days) in observed (OBS), control (CTR) and scenario (SCA) climates: regardless of circulation types (ALL), and for individual types separately (1–6)

	ALL	1	2	3	4	5	6
OBS	2.7	2.7	3.1	2.4	2.6	2.5	2.4
CTR	2.7	3.0	2.3	2.4	2.9	2.7	2.6
SCA	2.5	2.8	2.0	1.9	2.4	2.5	2.6

TABLE IX

Mean amplitudes of low-frequency circulation modes under heat waves. Shown are the minimum (MIN) and maximum (MAX) value from the eight stations, the value for the area-averaged temperature (AVG), and values for the control (CTR) and scenario (SCA) climates for the two threshold definitions (AP, AT)

Mode	MIN	MAX	AVG	CTR AP	CTR AT	SCA AP	SCA AT
1	0.582	0.813	0.701	0.347	0.336	0.144	0.155
2	0.375	0.576	0.466	0.118	0.187	0.080	0.085
3	0.184	0.333	0.323	0.273	0.297	0.042	0.041

6. Relationships between Heat Waves, Dry Spells and Circulation

In this section, we investigate which circulation conditions are associated with the occurrence of prolonged extreme events, and which conditions act against their formation. Heat waves and dry spells are related to circulation in two ways: First, the amplitudes of the circulation modes in both frequency bands are averaged over all the heat waves and dry spells. Second, the numbers of days in heat waves and dry spells are counted for individual circulation types separately. Indeed, causation cannot be proved this way. On the time scales discussed, however, one may assume that in general, circulation governs surface weather, although the opposite effect is also possible: For example, long-lasting high temperatures may support ridging in mid-troposphere.

6.1. MODES OF VARIABILITY

The observed heat waves are associated with positive amplitudes of all three low-frequency modes, the relationship with mode 1 being most intense as indicated by highest mean amplitudes (Table IX). This holds for individual stations as well as

TABLE X
Same as in Table IX except for synoptic-frequency modes

Mode	MIN	MAX	CTR AP	SCA AP
1	0.044	0.100	0.024	–0.003
2	–0.069	–0.017	–0.035	–0.010
3	–0.104	0.011	–0.031	0.001
4	–0.030	0.031	0.003	–0.004
5	–0.010	0.064	0.054	0.010

the area-averaged series. This means that conditions favourable for a heat wave to occur in south Moravia are positive 500 hPa height anomalies over southern Scandinavia (mode 1), southwest Europe (mode 2), and to a smaller extent over Greece and negative anomaly over Ireland (mode 3) (see Figure 5). This could be expected since all these conditions support an inflow of warm air from south and southwest into central Europe (modes 1 and 3) and/or the presence of a ridge or anticyclone over there (modes 1 and 2).

The linkage between low-frequency modes and heat waves in the control climate is considerably weaker. The effect of the Scandinavian anomaly (mode 1) is approximately halved and that of southwest-European anomaly (mode 2) becomes negligible. Only the relationship of mode 3 with heat waves is simulated with a correct intensity. The influence of circulation modes becomes negligible in the scenario climate because of an immense increase in heat waves occurrence.

The synoptic-frequency modes do not manifest any relation to the occurrence of heat waves (Table X). No effect of the synoptic-frequency modes appears in the control and scenario climates either.

The linkage with modes of variability is weaker for dry spells than for heat waves (Table XI). The only mode associated with the occurrence of dry spells is low-frequency mode 1, whose positive amplitude inhibits precipitation due to forming a ridge or anticyclone over central Europe. This link is pronounced more strongly for the area-averaged precipitation than at individual stations, but is reproduced too weak in the control climate. The synoptic-frequency modes have no effect on dry spells, the mean amplitudes not exceeding 0.05 in either climate analyzed (not shown).

6.2. CIRCULATION TYPES

The connection between circulation types and prolonged extreme events may be characterized by a ratio between the number of event-days (i.e., days within the heat waves or dry spells) classified with a particular type and the total number

TABLE XI
Same as in Table IX except for dry spells

Mode	MIN	MAX	AVG	CTR
1	0.314	0.546	0.658	0.269
2	0.088	0.194	0.159	0.128
3	–0.052	0.112	–0.140	–0.080

of event-days. However, such a quantity is not feasible because the types occur with different frequencies and the frequency of any single type may differ between climates, so a direct comparison among types and between climates would be impossible. Therefore, the above-defined ratio is divided by the relative frequency of the type in a particular climate (defined as a ratio of the number of days classified with that type and the total number of days). Such a coefficient quantifies a relative contribution of a particular circulation type to the occurrence of heat waves or dry spells: its value greater (less) than unity indicates that the heat waves or dry spells occur more (less) frequently under that type than if they were distributed in all types uniformly (i.e., if there were no association with circulation).

The values of the above defined coefficient for heat waves and dry spells at all stations and in the control and scenario climates are presented in Table XII. Despite a pronounced spatial variability, the effect of circulation types on the occurrence of heat waves and dry spells in the observed climate is obvious and in agreement with synoptic experience. The heat waves are favoured at all stations under warm anticyclonic types 2 and 6; situations with cyclonic conditions (type 3) and cool northwest cyclonic flow (type 5) occur during heat waves only exceptionally or not at all. The occurrence of heat waves is relatively low under cool northwest type 4, and close to the climatological expectation (except for the two westernmost highland stations) under zonal type 1. The intensity of association of heat waves in the area-averaged temperature series with circulation types is very close to that pooled over individual stations. The incidence of dry spells under different types is governed by their cyclonicity/anticyclonicity: The occurrence of dry spells is higher under anticyclonic types 2, 4 and 6 while is less frequent under zonal type 1 and cyclonic types 3 and 5. The area-averaged precipitation manifests a stronger connection of dry spells with circulation than the individual station series: The coefficient in Table XII for area-averaged precipitation is lower (higher) for dry (wet) types than the coefficient pooled over all stations.

The relative contribution of circulation types to the formation of heat waves and dry spells is changed in the control climate. The conditions under cool cyclonic types 3 and 5 remain entirely unfavourable for heat waves. However, the contribution of the other four types is levelled out, the difference between warm anticyclonic and cool or zonal types being neglected. Warm anticyclonic types

TABLE XII

Coefficient quantifying a relative contribution of circulation types to the occurrence of heat waves (top) and dry spells (bottom). For the definition of the coefficient see the text. The notation of columns is analogous to Table I

Circulation type	636	687	698	723	754	755	774	779	ALL	AVG	CTR AP	CTR AT	SCA AP	SCA AT
1	0.46	0.74	1.01	0.90	1.17	1.16	1.03	0.99	0.93	1.04	1.32	1.32	1.38	1.37
2	2.30	2.33	1.77	1.86	1.87	1.71	2.10	2.06	2.00	2.03	1.11	1.09	0.83	0.79
3	–	–	–	–	0.05	0.09	0.06	–	0.02	–	0.06	0.07	0.37	0.38
4	0.60	0.67	0.58	0.63	0.63	0.59	0.42	–	0.51	0.52	1.05	0.93	0.78	0.79
5	–	–	0.04	–	–	0.05	–	–	0.01	–	0.11	0.11	0.26	0.25
6	1.76	1.27	1.70	1.70	1.30	1.50	1.40	1.98	1.58	1.41	1.32	1.45	1.22	1.23

Circulation type	636	687	698	723	754	755	774	779	ALL	AVG	CTR
1	0.65	0.65	0.75	0.74	0.73	0.83	0.70	0.84	0.74	0.58	1.06
2	1.27	1.20	0.97	1.10	1.09	1.10	1.14	1.08	1.12	1.01	0.76
3	0.82	0.59	0.75	0.70	0.66	0.74	0.71	0.74	0.71	0.61	0.27
4	1.27	1.34	1.34	1.23	1.26	1.23	1.25	1.15	1.26	1.48	1.20
5	0.47	0.41	0.60	0.61	0.61	0.49	0.45	0.30	0.49	0.44	0.25
6	1.36	1.54	1.48	1.46	1.48	1.41	1.56	1.67	1.49	1.71	1.57

2 and 6 become less conducive to forming heat waves whereas the occurrence of heat waves under cooler situations, i.e., zonal type 1 and northwest type 4, is enhanced relative to the observed climate. Regarding dry spells, the model underestimates their occurrence under cyclonic situations (types 3 and 5) and type 2, and overestimates for zonal type 1.

The under- (over-) estimation of heat waves for warm anticyclonic (cool zonal and northwest) situations and the overestimation of dry spells for the zonal circulation type indicate that in the model, the advected air undergoes a more rapid transformation over the continent, losing its original properties more quickly. This means that the model air-mass transformation and local processes, most likely radiation, overweigh advection either because the advection is too weak or the transformation processes too strong.

In the scenario climate, the numbers of days in heat waves increase considerably (Table XII top). Consequently, their relation with circulation types weakens. In spite of this, the types least favourable for heat wave occurrence in the observed and control climates (cyclonic types 3 and 5) are also connected with the fewest events in the scenario climate.

7. Discussion

The results on the validation of heat waves are basically the same regardless of whether the GCM output is treated as a gridbox or gridpoint value, because only a marginal difference was found between the heat wave characteristics calculated from individual station values, and from areal means. We identified several deficiencies of the ECHAM3 GCM in simulating heat waves in south Moravia (southeast Czech Republic): Heat waves in the model are too long, appear later in the year, peak at higher temperatures, their numbers (as well as the numbers of tropical days) are underestimated in the beginning of summer (June, July) but overestimated in August, and fewer tropical days occur outside of heat waves.

The area-averaged and single station series yield very close characteristics of the duration of dry spells as well as similar shapes of annual cycles of the dry spells and dry days occurrence. The dry spells frequency and the percentage of dry days within dry spells, however, differ widely between the area-averaged and station series. The simulated precipitation resembles the areal average in the dry spells frequency, whereas in the percentage of dry days within dry spells, it approximates the station values. In the dry spells duration and annual cycle of dry spells and dry days, the simulation is far from both station and area-averaged values. We can therefore conclude that whatever the treatment of the simulated precipitation, dry spells are too long in the model and the annual cycle of their occurrence (as well as that of dry days) is deformed.

All these deficiencies arise as a direct result of a combination of ECHAM's errors in simulating surface temperature and precipitation on a daily scale, re-

ported recently (Nemešová and Kalvová, 1997; Kalvová and Nemešová, 1998; Nemešová et al., 1998), which include an overestimated persistence of temperature, a deformation of annual cycles of temperature and precipitation, and a distorted distribution of daily precipitation amounts. Since the errors in temperature persistence and annual cycles appear to be common to many models (cf. Buishand and Beersma, 1993; Mearns et al., 1995; Kalvová and Nemešová, 1997; Smith and Pitts, 1997), the characteristics of heat waves and dry spells are unlikely to be reproduced realistically by other models either.

In contrast to temperature and precipitation, large-scale circulation at the 500 hPa level is simulated relatively successfully by the ECHAM GCM. Modes of variability (in both frequency bands) are reproduced very well. The occurrence of some circulation types is estimated rather poorly. This is especially true for the type with an extensive ridge over most of Europe for which the frequency in the control simulation is half of that observed. There is no general bias in the persistence of circulation types, some of them being more persistent in the control climate, some of them less persistent. This is in contrast to surface temperature, the persistence of which has been shown to be exaggerated in the model.

The occurrence of heat waves and dry spells (prolonged events) is associated with distinctive patterns of large-scale circulation. In particular, the heat waves (dry spells) tend to occur under positive amplitudes of all (one) of the three low-frequency circulation modes. The association of circulation modes with dry spells is weaker than with heat waves, but still important. The synoptic-frequency modes manifest, on the other hand, no connection with prolonged events. The probability that a prolonged event will appear differs considerably among circulation types. Some of the types provide a favorable background for prolonged events to occur while under other types prolonged events are observed rather exceptionally or almost not at all. These findings are in accord with results of Huth (1997b) who found on different datasets that temperature is associated with circulation more tightly than precipitation, the bulk of the association being concentrated in low-frequency circulation modes.

Since circulation and its persistence are reproduced well while the simulation of prolonged events is far from being acceptable, it becomes obvious that what is simulated incorrectly must be the link between circulation and surface climate elements. The analysis presented here proves this anticipation. The influence of circulation on prolonged events is considerably weaker in the control climate than in the observed. This is manifested by the average amplitudes of low-frequency modes being closer to zero under prolonged events as well as a more even distribution of prolonged events among individual circulation types. This means that in the control climate, the flow configuration, characterized by the circulation type, has less association with prolonged events than in the observed. In other words, the advected air loses its original properties too quickly, the air-mass transformation playing too important a role. This leads us to formulating the hypothesis that either

the transformation and local processes, most likely radiative heating, are too strong in the model or the model advection is too weak.

In the scenario climate, the characteristics of heat waves change dramatically. It should be noted that the increase in mean maximum temperature by a rather realistic value of about 4.5 °C leads to a five-fold increase in the frequency of tropical days, and to a great increase in the extremity of heat waves (in their number, duration and peak temperature). In spite of it, the heat waves occur in the same months as in the control climate (i.e., June to September) and do not spread earlier in spring and later in autumn.

To conclude, the ECHAM3 GCM simulates large-scale circulation features successfully. However, because of an inadequate linkage between circulation and surface climate, the model fails in reproducing many characteristics of heat waves and dry spells. Only little confidence can then be placed in their properties in the scenario climate. Therefore, instead of a direct use of GCM-produced daily series, the incremental scenarios were created for precipitation in assessments of climate change impacts in the Czech Republic, whereas for temperature, the monthly warming rates indicated by ECHAM were disaggregated into daily series with a weather generator (Nemešová et al., 1999). Based on these scenarios, impacts on wheat and maize yields (Dubrovský et al., 2000; Žalud et al., 1999) and hydrological regimes in small catchments (Buchtele et al., 1999) were assessed using the crop growth and hydrological models.

8. General Implications for Climate Impact Studies

In the end, we would like to raise several methodological issues, related to using GCM outputs for assessing climate change impacts that may be of a general interest.

Validation. Before using outputs of GCM perturbed runs in climate change impact studies, i.e., before constructing climate change scenarios (projections), a detailed validation of a GCM control run should be performed. Such a validation should be fitted to the task to be dealt with. For example, the discussion in the Introduction implies that a realistic simulation of heat waves and dry spells is definitely of crucial importance in crop growth modelling. The sensitivity of crop yields to the persistence of daily temperature and precipitation was proved in the modelling study by Dubrovský (1998). The realistic simulation of dry spells is no doubt important in hydrological modelling as well, especially for small river basins. Therefore, proving that the annual means or seasonal cycles are simulated successfully without examining persistence is insufficient if one wants to produce a scenario for assessing agricultural and hydrological impacts.

Gridpoint vs. gridbox issue. The climate of the control run of a GCM must be validated against the appropriate observed quantities. The study suggests that for some characteristics, the validation against area-representative values is feasible

while for the others, the validation should be done against station data. What to compare the GCM control run with must be made clear before the considerations on the GCM's validity are formulated. The input into local impact models (such as crop-growth models) of the variables that are simulated by a GCM as area-representative rather than local values may not be adequate, and other methods of their specification should be sought.

Plausibility of future climate. Confidence can be placed in the scenario climate only if the variables (phenomena) of interest are reproduced realistically in the control climate. Inversely, if a model is successful in simulating the present climate, then even an unrealistic future climate (unrealistic from the present point of view, indeed), produced by that model, must be treated as a real possibility of future climate development.

Downscaling. The temperatures and precipitation produced by the ECHAM3 GCM have been shown to be unsuitable for assessing impacts for which the time structure of daily temperature and precipitation series is important. However, large-scale upper-air variables (both circulation and temperature) are simulated fairly well (Huth and Kyselý, 1999). This gap between what GCM outputs can provide and what is needed for impact assessments is inherent in GCMs (e.g., von Storch, 1995) and may be bridged by statistical downscaling and/or stochastic modelling methods (e.g., Dubrovský, 1997; Semenov and Barrow, 1997). The former are based on applying the observed relationships between large-scale upper-air fields and local climate variables to the simulated large-scale fields; the latter replicate the stochastic structure of observed time series. There is good reason to believe that the downscaled and stochastically modelled variables will be a more accurate representation of future climate. More specifically, heat waves and dry spells obtained from downscaled temperature and precipitation values are expected to be in better agreement with the observations than those from a direct GCM output.

Acknowledgements

This study was supported by the Grant Agency of the Czech Republic, contracts 205/96/1669 and 205/96/1670, and by the Grant Agency of the Academy of Sciences, contract A3060605. Thanks are due to two anonymous reviewers and Prof. S. H. Schneider for their insightful and helpful reviews and comments and Dr. I. Nemešová for comments on an earlier version of the manuscript. Mrs. E. Lhotková assisted in drawing the figures.

References

Acock, B. and Acock, M. C.: 1993, 'Modeling Approaches for Predicting Crop Ecosystem Responses to Climate Change', in *International Crop Science*, Vol. I, Crop Science Society of America, Madison, pp. 299–306.

Airey, M. and Hulme, M.: 1995, 'Evaluating Climate Model Simulations of Precipitation: Methods, Problems and Performance', *Progr. Phys. Geogr.* **19**, 427–448.

Blackmon, M. L. and Lau, N.-C.: 1980, 'Regional Characteristics of the Northern Hemisphere Wintertime Circulation: A Comparison of the Simulation of a GFDL General Circulation Model with Observations', *J. Atmos. Sci.* **37**, 497–514.

Buchtele, J., Buchtelová, M., Fořtová, M., and Dubrovský, M.: 1999, 'Runoff Changes in Czech River Basins – the Outputs of Rainfall-Runoff Simulations Using Different Climate Change Scenarios', *J. Hydrol. Hydromech.* **47**, 180–194.

Buishand, T. A. and Beersma, J. J.: 1993, 'Jackknife Tests for Differences in Autocorrelation between Climate Time Series', *J. Climate* **6**, 2490–2495.

Cavestany, D., El Wishy, A. B., and Foote, R. H.: 1985, 'Effect of Season and High Environmental Temperature on Fertility of Holstein Cattle', *J. Dairy Sci.* **68**, 1471–1478.

Changnon, S. A., Kunkel, K. E., and Reinke, B. C.: 1996, 'Impacts and Responses to the 1995 Heat Wave: A Call to Action', *Bull. Amer. Meteorol. Soc.* **77**, 1497–1506.

DKRZ, 1993: 'The ECHAM3 Atmospheric General Circulation Model', Report No. 6, Deutsches Klimarechenzentrum, Hamburg, p. 184.

Dubrovský, M.: 1997, 'Creating Daily Weather Series with Use of the Weather Generator', *Environmetrics* **8**, 409–424.

Dubrovský, M.: 1998, 'Estimating Climate Change Impacts on Crop Yields with Use of Crop Growth Model and Weather Generator', in *Proceedings of the 14th Conference on Probability and Statistics in Atmospheric Science*, American Meteorological Society, Phoenix, pp. 86–87.

Dubrovský, M., Žalud, Z., and Št'astná, M.: 2000, 'Sensitivity of CERES-Maize Yields to Statistical Structure of Daily Weather Series', *Clim. Change*, in press.

Furquay, J. W.: 1989, 'Heat Stress as it Affects Animal Production', *J. Animal Sci.* **52**, 164–174.

Gregory, J. M., Mitchell, J. F. B., and Brady, A. J.: 1997, 'Summer Drought in Northern Midlatitudes in a Time-Dependent CO_2 Climate Experiment', *J. Climate* **10**, 662–686.

Hennessy, K. J. and Pittock, A. B.: 1995, 'Greenhouse Warming and Threshold Temperature Events in Victoria, Australia', *Int. J. Climatol.* **15**, 591–612.

Hennessy, K. J., Gregory, J. M., and Mitchell, J. F. B.: 1997, 'Changes in Daily Precipitation under Enhanced Greenhouse Conditions', *Clim. Dyn.* **13**, 667–680.

Huth, R.: 1997a, 'Continental-Scale Circulation in the UKHI GCM', *J. Climate* **10**, 1545–1561.

Huth, R.: 1997b, 'Potential of Continental-Scale Circulation for the Determination of Local Daily Surface Variables', *Theor. Appl. Climatol.* **56**, 165–186.

Huth, R. and Kyselý, J.: 1999, 'Constructing Site-Specific Climate Change Scenarios on a Monthly Scale Using Statistical Downscaling', *Theor. Appl. Climatol.*, in press.

Joubert, A. M., Mason, S. J., and Galpin, J. S.:, 1996, 'Droughts over Southern Africa in a Doubled CO_2 Climate', *Int. J. Climatol.* **16**, 1149–1156.

Kalkstein, L. S. and Smoyer, K. E.: 1993, 'The Impact of Climate Change on Human Health: Some International Implications', *Experientia* **49**, 969–979.

Kalvová, J. and Nemešová, I.: 1997, 'Projections of Climate Change for the Czech Republic', *Clim. Change* **36**, 41–64.

Kalvová, J. and Nemešová, I.: 1998, 'Estimating Autocorrelations of Daily Extreme Temperatures in Observed and Simulated Climates', *Theor. Appl. Climatol.* **59**, 151–164.

Karl, T. R. and Knight, R. W.: 1997, 'The 1995 Chicago Heat Wave: How Likely Is a Recurrence?', *Bull. Amer. Meteorol. Soc.* **78**, 1107–1119.

Katz, R. W. and Brown, B. G.: 1992, 'Extreme Events in a Changing Climate: Variability is More Important than Averages', *Clim. Change* **21**, 289–302.

Kirschbaum, M. U. F.: 1996, 'Ecophysiological, Ecological, and Soil Processes in Terrestrial Ecosystems: A Primer on General Concepts and Relationships', in Watson, R. T., Zinyowera, M. C., Moss, R. H., and Dokken, D. J. (eds.), *Climate Change 1995. Impacts, Adaptations and Mitigation of Climate Change: Scientific-Technical Analyses*, Cambridge University Press, Cambridge, U.K., pp. 57–74.

Kunst, A. E., Looman, C. W. N., and Mackenbach, J. P.: 1993, 'Outdoor Air Temperature and Mortality in The Netherlands: A Time-Series Analysis', *Amer. J. Epidemiol.* **137**, 331–341.

Kyselý, J. and Kalvová, J.: 1998, 'Heat Waves in South Moravia in 1961–1990', *Meteorol. zprávy* **51**, 65–72 (in Czech).

Mason, S. J. and Joubert, A. M.: 1997, 'Simulated Changes in Extreme Rainfall over Southern Africa', *Int. J. Climatol.* **17**, 291–301.

Mearns, L. O., Giorgi, F., McDaniel, L., and Shields, C.: 1995, 'Analysis of Variability and Diurnal Range of Daily Temperature in a Nested Regional Climate Model: Comparison with Observations and Doubled CO_2 Results', *Clim. Dyn.* **11**, 193–209.

Nemešová, I. and Kalvová, J.: 1997, 'On the Validity of ECHAM-Simulated Daily Extreme Temperatures', *Studia Geoph. Geod.* **41**, 396–406.

Nemešová, I., Kalvová, J., Buchtele, J., and Klimperová, N.: 1998, 'Comparison of GCM-Simulated and Observed Climates for Assessing Hydrological Impacts of Climate Change', *J. Hydrol. Hydromech.* **46**, 237–263.

Nemešová, I., Kalvová, J., and Dubrovský, M.: 1999, 'Climate Change Projections Based on GCM-Simulated Daily Data', *Studia Geoph. Geod.* **43**, 201–222.

Osborn, T. J. and Hulme, M.: 1998, 'Evaluation of the European Daily Precipitation Characteristics from the Atmospheric Model Intercomparison Project', *Int. J. Climatol.* **18**, 505–522.

Palutikof, J. P., Winkler, J. A., Goodess, C. M., and Andresen, J. A.: 1997, 'The Simulation of Daily Temperature Time Series from GCM Output. Part I: Comparison of Model Data with Observations', *J. Climate* **10**, 2497–2513.

Portman, D. A., Wang, W.-C., and Karl, T. R.: 1992, 'Comparison of General Circulation Model and Observed Regional Climates: Daily and Seasonal Variability', *J. Climate* **5**, 343–353.

Reed, D. N.: 1986, 'Simulation of Time Series of Temperature and Precipitation over Eastern England by an Atmospheric General Circulation Model', *J. Climatol.* **6**, 233–253.

Reilly, J.: 1996, 'Agriculture in a Changing Climate: Impacts and Adaptation', in Watson, R. T., Zinyowera, M. C., Moss, R. H., and Dokken, D. J. (eds.), *Climate Change 1995. Impacts, Adaptations and Mitigation of Climate Change: Scientific-Technical Analyses*, Cambridge University Press, Cambridge, U.K., pp. 427–467.

Risbey, J. S. and Stone, P. H.: 1996, 'A Case Study of the Adequacy of GCM Simulations for Input to Regional Climate Change Assessments', *J. Climate* **9**, 1441–1467.

Robinson, P. J., Samel, A. N., and Madden, G.: 1993, 'Comparisons of Modelled and Observed Climate for Impact Assessments', *Theor. Appl. Climatol.* **48**, 75–87.

Schubert, S.: 1998, 'Downscaling Local Extreme Temperature Changes in South-Eastern Australia from the CSIRO Mark2 GCM', *Int. J. Climatol.* **18**, 1419–1438.

Semenov, M. A. and Barrow, E. M.: 1997, 'Use of a Stochastic Weather Generator in the Development of Climate Change Scenarios', *Clim. Change* **35**, 397–414.

Skelly, W. C. and Henderson-Sellers, A.: 1996, 'Grid Box or Grid Point: What Type of Data Do GCMs Deliver to Climate Impacts Researchers?', *Int. J. Climatol.* **16**, 1079–1086.

Smith, J. B. and Pitts, G. J.: 1997, 'Regional Climate Change Scenarios for Vulnerability and Adaptation Assessments', *Clim. Change* **36**, 3–21.

Thatcher, W. W.: 1974, 'Effects of Season, Climate and Temperature on Reproduction and Lactation', *J. Dairy Sci.* **57**, 360–368.

von Storch, H.: 1995, 'Inconsistencies at the Interface of Climate Impact Studies and Global Climate Research', *Meteorol. Z., N.F.* **4**, 72–80.

Žalud, Z., Dubrovský, M., and Šťastná, M.: 1999, 'Climate Change Impacts on Grain Yields Assessed by Crop Growth Models CERES-Maize and CERES-Wheat', *Agric. For. Meteorol.*, submitted.

Zwiers, F. W. and Kharin V. V.: 1998, 'Changes in the Extremes of the Climate Simulated by CCC GCM2 under CO_2 Doubling', *J. Climate* **11**, 2200–2222.

(Received 28 August 1998; in revised form 28 October 1999)